



## Drivers of declining sea ice in the Arctic winter: A tale of two seas

Jennifer A. Francis<sup>1</sup> and Elias Hunter<sup>1</sup>

Received 13 June 2007; revised 25 July 2007; accepted 10 August 2007; published 14 September 2007.

[1] While the summer perennial Arctic sea ice has declined markedly in recent decades, the maximum extent of the winter ice cover had decreased only slightly, until the past few years when it also receded dramatically. This investigation reveals that the timing of maximum extent varies greatly, and the drivers of ice-edge location differ strikingly between two of the areas where it varies most: the Bering and Barents Seas. Between 1979 and 2005 in the Bering Sea, the ice edge is influenced mainly by anomalies in easterly winds associated with the Aleutian Low, which was particularly strong during the 1980s. The Barents Sea ice edge, in contrast, is driven primarily by two factors: anomalies in sea-surface temperature, particularly close in time to the maximum extent, and by southerly wind (from the south) anomalies integrated back to mid- and early winter. The hemispheric-mean decline in winter ice extent is due in large part to increasing sea-surface temperatures in the Barents Sea and adjoining waters, which are consistent with increased concentrations of greenhouse gases. **Citation:** Francis, J. A., and E. Hunter (2007), Drivers of declining sea ice in the Arctic winter: A tale of two seas, *Geophys. Res. Lett.*, 34, L17503, doi:10.1029/2007GL030995.

### 1. Introduction

[2] The decline in Arctic sea ice during recent decades is dramatic, particularly during summer when observed extent decreased by  $\sim 10\%$  per decade [Stroeve *et al.*, 2005; Comiso, 2006a]. The extent of the winter ice cover, however, had not changed appreciably – until recently. Figure 1 presents satellite-derived sea ice concentrations from the National Snow and Ice Data Center. It illustrates the relatively slow decline in ice cover until the late 1990s during March, when ice is typically most extensive, followed by a precipitous decrease through 2006. Change in winter ice extent was also documented by Comiso [2006b] using visible and infrared satellite data. He found that hemispheric-mean winter ice loss corresponded with increasing surface temperatures and anomalous wind patterns, concluding that a combination of atmospheric warming and wind-driven ice motion likely contributed to the observed changes. Because rapid Arctic warming is believed to result primarily from increased greenhouse gas concentrations, Comiso surmised that observed winter ice loss is a clear indication of anthropogenic climate change.

[3] This investigation builds on the observations of Comiso [2006b] by quantitatively investigating the drivers of varying winter ice cover. In much of the Arctic Ocean,

sea ice forms during autumn until it reaches a coast, and thus can extend no farther. In the Barents and Bering Seas, however, the ice edge can move freely in response to the dynamic and thermodynamic forces acting upon it, and these two areas account for much of the variability in hemispheric winter ice-cover. Winter ice extent is of particular interest as an indicator of the so-called ice-albedo feedback. When an unusually large amount of ice melts during the spring and summer, additional open water is exposed, which allows more solar energy to be absorbed into the ocean. If enough additional energy is absorbed so that freezing in the marginal seas is delayed and ultimately reduced during winter, then sea ice at the beginning of the following spring will be thinner and more easily melted away during summer. Because so much perennial sea ice has been lost in recent years, Serreze and Francis [2006] and Lindsay and Zhang [2005] have speculated that the ice-albedo feedback may now be operating, explaining the continued loss of summer ice even though the large-scale atmospheric circulation over the Arctic has returned to its more normal anticyclonic pattern after a period of anomalously cyclonic flow during the late 1980s and early 1990s [Rigor and Wallace, 2004]. The abrupt loss of winter ice in recent years is worrisome evidence supporting this speculation, thus a clearer picture is needed of the mechanisms driving variability in the winter-maximum ice-edge location.

### 2. New Approach, New Information

[4] Anomalies in winds and thermodynamic forcing accumulated over the months prior to maximum ice extent are likely the primary drivers of variability in ice edge location. The relative contributions of these effects are investigated using new satellite products derived from satellite sounding instruments, which include downward longwave fluxes (DLF) and zonal and meridional winds (U,V). A similar approach was used by Francis and Hunter [2006] to investigate causes of summer-minimum sea ice variability. The atmospheric information is combined with anomalies in sea-surface temperature (SST) of the open ocean southward of the ice edge to represent the influence of heating by the ocean.

[5] The edge of compact sea ice, defined here as the southernmost latitude of 50% concentration determined with daily passive microwave satellite data [Meier *et al.*, 2006], is identified in the Barents and Bering Seas along four-degree-wide longitude bands centered on 30°E and 190°E, respectively (Figure 2). The distance from the edge southward to a fixed position is measured, and the date of maximum annual ice extent establishes the reference point from which forcing anomalies are integrated backward in time. Anomalies in maximum ice extent (hereafter MaxIA) are calculated by subtracting the position for each year from the 27-year mean position in that region.

<sup>1</sup>Institute of Marine and Coastal Sciences, Rutgers University, New Brunswick, New Jersey, USA.

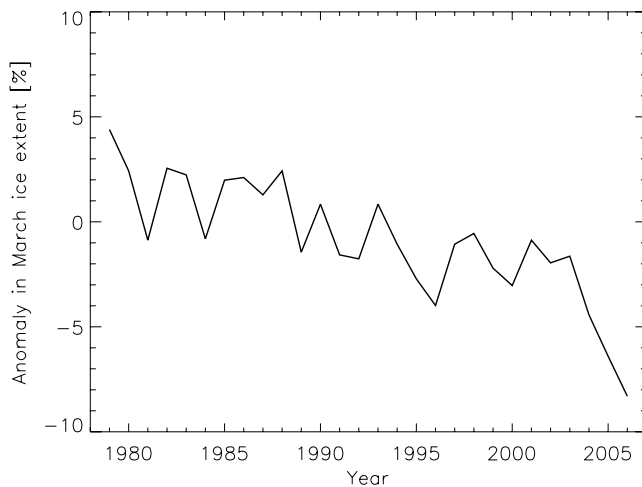


**Figure 1.** Monthly anomalies in Northern Hemisphere sea ice extent during March, expressed in percentage of mean extent during 1979 to 2000 (data from <http://www.nsidc.org>).

[6] Time series of anomalies in the forcing parameters are calculated from daily-mean values using slightly different methods in each region because of their geographic differences. In the Barents (Bering) Sea, anomalies in DLF and winds are calculated within a 400-km-radius (200-km-radius) circle located 450 (250) km north of the ice edge on each day. As the ice-edge moves, so does the subsetting circle, ensuring that the anomalies are located over the pack ice and minimally affected by the substantial discontinuity in temperature at the ice edge. The Bering Sea region is smaller to allow it to shift into the Bering Strait with little land influence. The SST anomalies in the Barents (Bering) Sea are calculated within a fixed 400-km-radius circle centered at 70°N, 5°E (57.5°N, 177.5°E), which is ice-free, clear of landmasses, and near the ice edge. Time series in all parameters are smoothed using a 10-day running mean, then 10-day anomalies are calculated as the difference from the 27-year mean for that 10-day period. Anomalies are integrated backward to 90 days from the date of maximum extent and normalized by their standard deviation, then correlations are calculated. Daily mean DLFs over the pack ice from 1979 to 2005 are derived from the TIROS Operational Vertical Sounder (TOVS) [Francis, 1997]. Near-surface winds in the Barents Sea are derived from TOVS [Francis *et al.*, 2005]. Winds in the Bering Sea as well as sea-surface temperatures in both locations are obtained from the National Center for Environmental Predictions's reanalysis [Kistler *et al.*, 2001].

### 3. What Drives Winter Ice-Edge Variability?

[7] Time series of the anomalies in maximum extent and the dates of occurrence in the Barents and Bering Seas are presented in Figure 3. The mean latitude and date of annual-maximum ice extent in the Barents (Bering) Sea are 75.6°N, March 19th (58.1°N, March 11th). Large interannual variability is evident in both the position of the southernmost ice edge and the date at which it occurs. The MaxIA has progressed steadily northward in the Barents

Sea (28 km dec<sup>-1</sup>, 90% statistical confidence) since 1979, while its date has occurred later (5.5 days dec<sup>-1</sup>), albeit not significantly so. In contrast, the ice-edge position in the Bering Sea appears to have migrated southward from 1979 through the mid-1990s, but thereafter exhibits a marked northward retreat at a rate of approximately 120 km dec<sup>-1</sup>. The tendency in the date of maximum extent is slightly earlier (-3.1 days dec<sup>-1</sup>), but this trend is also not statistically significant.

[8] The relative contributions of integrated anomalies in forcing parameters that drive ice-edge variability is investigated with multiple regression analysis, as tests for the applicability of this approach revealed no violations of regression theory. Histograms in Figure 4 depict the variance in MaxIAs attributable to anomalies in each forcing parameter, integrated from zero to 90 days prior to the date of maximum ice extent. The bar height indicates the total variance accounted for, while colored sections denote statistically significant (>90%) contributions by each parameter.

[9] The most striking aspect of the histograms for the two regions is their marked dissimilarity. In the Barents Sea, the lion's share of the variance is attributable to anomalies in the SST (red). This influence decreases with increasing integration time, being replaced by anomalies in southerly (from the south) winds (V, blue). The downwelling long-wave flux anomalies also play a minor role during mid-winter. In the Barents Sea, therefore, the mechanisms controlling the winter-maximum ice edge appear to be dominated by a combination of warmer surface waters near the ice edge, and by anomalous meridional winds, which can mechanically force the ice and/or advect warmer (colder) air from the south (north).

[10] In the Bering Sea, a very different story emerges. Among the four parameters used in this investigation, anomalies in the zonal wind account for nearly all of the ice-edge variability. Easterly (from the east) wind anomalies correspond with retreating MaxIAs. This is consistent with

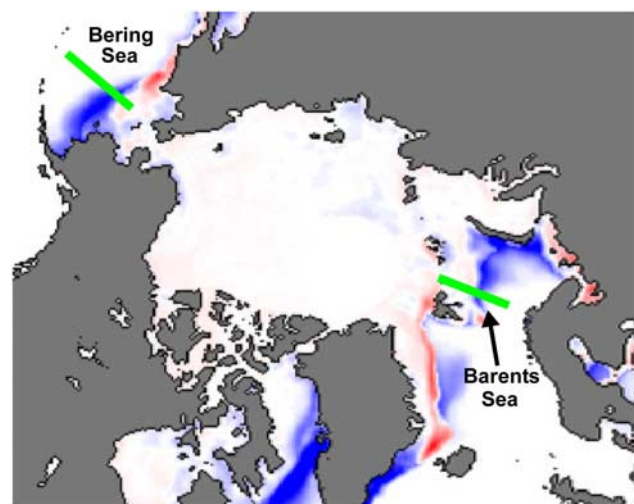


**Figure 2.** Anomalies in sea ice concentration during March 2005 derived from passive microwave satellite data by NSIDC (2006); losses (increases) shown in blue (red). The regions of analysis along longitudes 30°E (Barents) and 190°E (Bering) are marked with green lines.

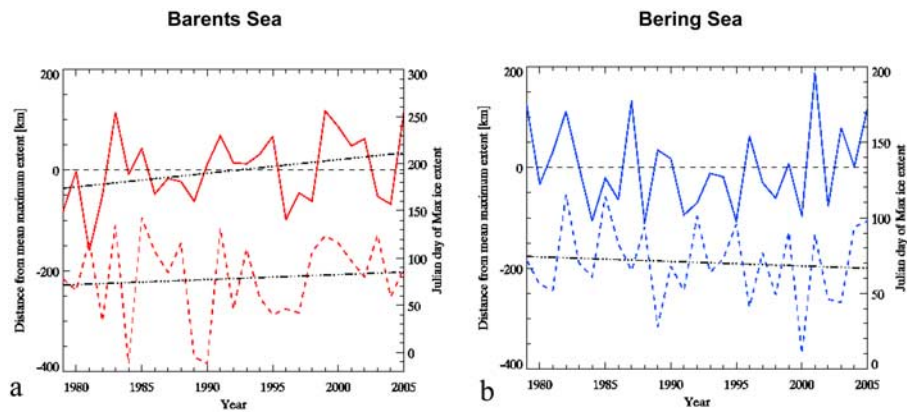


**Figure 3.** Time series of maximum winter ice-edge extent anomalies (solid) in km north of the mean location during 1979–2005, and Julian day of maximum ice extent (dashed) expressed relative to Jan. 1 of each year for the (a) Barents and (b) Bering seas. Slope of anomalies in ice extent in the Barents Sea is  $28 \text{ km dec}^{-1}$  (sig. at 90% confidence). Changes in timing of maximum ice extent are  $5.5 \text{ days dec}^{-1}$  and  $-3.1 \text{ days dec}^{-1}$  for the Barents and Bering seas, but the trends are not statistically significant. After 1995 in the Bering Sea, the ice edge location trend is  $123 \text{ km dec}^{-1}$ , but with only an 83% confidence level.

theory and observations that sea ice moves to the right of the geostrophic wind direction in the northern hemisphere [e.g., Colony and Thorndike, 1984]. Stabeno and Overland [2001] also speculated that changes in wind patterns in the Bering Sea area are likely the causal mechanisms for recent

variability in sea ice extent, which is further supported by Ukita *et al.* [2007].

[11] The intriguing shift in trend from a decreasing to increasing retreat in the ice edge position evident in the Bering Sea (Figure 3b) is investigated by splitting the time series into two intervals: 1979 to 1994 and 1995 to 2005.

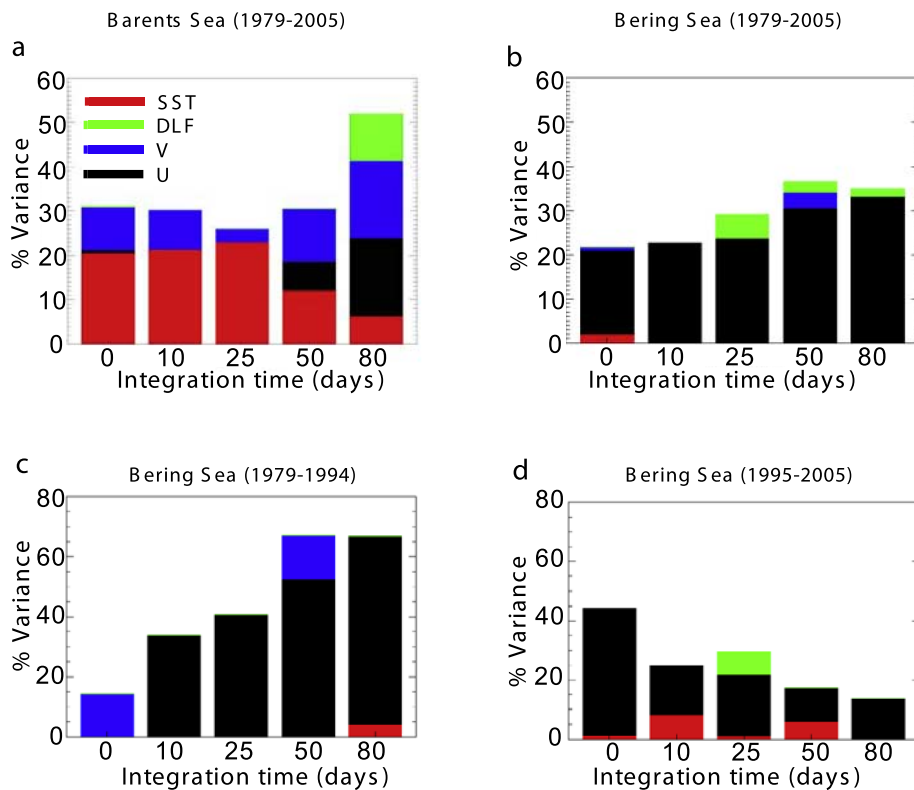


**Figure 4.** Percentage of variance in annual maximum ice-edge location accounted for by anomalies in winds, downwelling longwave flux, and sea-surface temperatures in the (a) Barents and (b) Bering seas for 1979–2005, and the Bering Sea from (c) 1979–1994 and (d) 1995–2005. Note difference in scale of y-axis in Figures 4c and 4d. Anomalies are integrated backward in time beginning at date of annual maximum extent from 0 to 90 days.

Figures 4c and 4d present the corresponding pair of histograms for each interval. In the earlier period, the mid-winter easterly wind anomalies account for about two thirds of the variance in MaxIAs. In the later interval, in contrast, east winds in late winter play the primary role, albeit less of the variance is accounted for. This result appears to be consistent with the behavior of the Pacific Decadal Oscillation (PDO) during the past few decades. In the earlier period, the winter PDO was in a predominantly positive phase, which is associated with a stronger Aleutian Low pressure center and stronger east winds in the Bering Sea [Mantua *et al.*, 1997]. After 1995 the PDO index was more neutral (<http://www.beringclimate.noaa.gov/>), leading to more variable winds and weaker correlations between easterly wind anomalies and the ice-edge location.

#### 4. Conclusions

[12] New satellite-derived sources of information are brought to bear on identifying the causes of recent losses in Arctic sea ice at the time of maximum extent in winter. While in much of the Arctic Ocean the winter ice extent is bounded by coastlines, in the Barents and Bering Seas the ice is relatively free to respond to changing atmospheric and oceanic conditions. These areas are also some of the most biologically productive oceanic regions in the world, thus major changes in the physical system will have profound effects on organisms that dwell there.

[13] This investigation combines 27 years of downwelling longwave radiation fluxes and wind fields derived from satellite sounding instruments with sea-surface temperatures from the NCEP reanalysis. A multiple regression analysis of anomalies in these forcing parameters against variability in satellite-derived ice-edge location suggests that the maximum ice extent responds to very different forcing parameters in the two seas. In the Bering Sea the ice-edge location appears to be governed nearly completely by anomalies in the flow around the Aleutian Low. When this semipermanent feature is strong, the ice edge is influenced primarily by zonal wind anomalies. This observation is generally consistent with the behavior of the PDO index, which was predominantly positive during the 1980s and corresponded with larger amounts of ice-edge variance being attributable to easterly wind anomalies (Figures 4c and 4d). The lack of correlation between ice-edge location and SSTs is consistent with the weak connection between the N. Pacific Drift current and the highly variable surface flows in the Bering Sea [e.g., Stabeno *et al.*, 1999].

[14] The maximum ice extent in the Barents Sea, in contrast, appears to be controlled primarily by anomalies in SSTs during the late winter as well as by meridional wind anomalies integrated back in time to mid- and early winter. The strong influence of SSTs on winter ice is consistent with the direct connection between the Barents Sea and the N. Atlantic and Norwegian Currents [e.g., Mork, 1981]. Sea surface temperatures in this region have increased substantially during winter in recent decades [e.g., Comiso, 2006b], which supports the SST influence identified in this investigation. The warming in the Barents Sea and adjoining waters is consistent with modeling studies linking increased concentrations of greenhouse gases with a warmer N. Atlantic Ocean [e.g., Hoerling *et al.*, 2001].

[15] The drivers of the winter-maximum ice edge identified in this investigation stand in stark contrast to the drivers of the summer-minimum perennial ice extent shown by Francis and Hunter [2006], which were dominated by anomalies in the downwelling longwave radiation flux. The winter ice in the Barents and Bering seas is thinner and more mobile than perennial or land-fast ice, resulting in an enhanced sensitivity to regional atmospheric and oceanic circulation features. As the oceans continue to warm and storminess increases in response to increasing concentrations of greenhouse gases, as predicted by state-of-the-art global climate models [Chapman and Walsh, 2007], winter ice extent will likely also continue to retreat northward, although the drivers will vary in different locations. Losses of perennial sea ice may be accelerated by the consequent reduction in ice volume at the beginning of the melt season, and normal life cycles of marine organisms will be profoundly disrupted.

[16] **Acknowledgments.** This work was funded by grants from NSF (ARC-0628818 and ARC-0240791), NASA (NAGW-2407 and NAG5-4908), and DOE (DE-FG02-02ER63313). We are grateful to A. Schweiger and M. Ortmeier for processing the TOVS data, and to the anonymous reviewers for their helpful suggestions.

#### References

- Chapman, W. L., and J. E. Walsh (2007), Simulations of arctic temperature and pressure by global coupled models, *J. Clim.*, *20*, 609–632.
- Colony, R. L., and A. Thorndike (1984), An estimate of the mean field of Arctic sea ice motion, *J. Geophys. Res.*, *89*, 10,623–10,629.
- Comiso, J. C. (2006a), Arctic warming signals from satellite observations, *Weather*, *61*, 70–76.
- Comiso, J. C. (2006b), Abrupt decline in the Arctic winter sea ice cover, *Geophys. Res. Lett.*, *33*, L18504, doi:10.1029/2006GL027341.
- Francis, J. A. (1997), A method to derive downwelling longwave fluxes at the Arctic surface from TOVS data, *J. Geophys. Res.*, *102*, 1795–1806.
- Francis, J. A., and E. Hunter (2006), New insight into the disappearing Arctic sea ice, *Eos Trans. AGU*, *87*, 509.
- Francis, J. A., E. Hunter, J. R. Key, and X. Wang (2005), Clues to variability in Arctic minimum sea ice extent, *Geophys. Res. Lett.*, *32*, L21501, doi:10.1029/2005GL024376.
- Hoerling, M. P., J. W. Hurrell, and T. Xu (2001), Tropical origins for recent North Atlantic climate change, *Science*, *292*, 90–92, doi:10.1126/science.1058582.
- Kistler, R., et al. (2001), The NCEP-NCAR 50-year reanalysis: Monthly means CD-ROM and documentation, *Bull. Am. Meteorol. Soc.*, *82*, 247–268.
- Lindsay, R. W., and J. Zhang (2005), The thinning of Arctic sea ice, 1988–2003: Have we reached the tipping point?, *J. Clim.*, *18*, 4879–4895.
- Mantua, N. J., S. R. Hare, Y. Zhang, J. M. Wallace, and R. C. Francis (1997), A Pacific interdecadal climate oscillation with impacts on salmon production, *Bull. Am. Meteorol. Soc.*, *78*, 1069–1079.
- Meier, W., F. Fetterer, K. Knowles, M. Savoie, and M. J. Brodzik (2006), Sea ice concentrations from Nimbus-7, SMMR, and DMSP SSM/I passive microwave data (1979–2005), Natl. Snow and Ice Data Cent., Boulder, Colo.
- Mork, M. (1981), Circulation phenomena and frontal dynamics of the Norwegian Coastal Current, *Philos. Trans. R. Soc. London, Ser. A*, *302*, 635–647.
- Rigor, I. G., and J. M. Wallace (2004), Variations in the age of Arctic sea ice and summer sea-ice extent, *Geophys. Res. Lett.*, *31*, L09401, doi:10.1029/2004GL019492.
- Serreze, M. C., and J. A. Francis (2006), The Arctic amplification debate, *Clim. Change*, *76*, 241–264, doi:10.1007/s10584-005-9017-y.
- Stabeno, P. J., and J. E. Overland (2001), The Bering Sea shifts toward an earlier spring transition, *Eos Trans. AGU*, *82*, 317.
- Stabeno, P. J., J. D. Schumacher, and K. Ohtani (1999), The physical oceanography of the Bering Sea: A summary of physical, chemical, and biological characteristics, and a synopsis of research on the Bering Sea, in *Dynamics of the Bering Sea, A Summary of Physical, Chemical, and Biological Characteristics, and a Synopsis of Research on the Bering Sea*, edited by T. R. Loughlin and K. Ohtani, pp. 1–28, Univ. of Alaska Sea Grant, Fairbanks.

Stroeve, J. C., M. C. Serreze, F. Fetterer, T. Arbetter, W. Meier, J. Maslanik, and K. Knowles (2005), Tracking the Arctic's shrinking ice cover: Another extreme September minimum in 2004, *Geophys. Res. Lett.*, 32, L04501, doi:10.1029/2004GL021810.

Ukita, J., M. Honda, H. Nakamura, Y. Tachibana, D. J. Cavalieri, C. L. Parkinson, H. Koide, and K. Yamamoto (2007), Northern Hemisphere sea

ice variability: Lag structure and its implications, *Tellus, Ser. A*, 59, 261–272, doi:10.1111/j.1600-0870.2006.00223.x.

---

J. A. Francis and E. Hunter, Institute of Marine and Coastal Sciences, Rutgers University, 71 Dudley Road, New Brunswick, NJ 08901, USA. (francis@imcs.rutgers.edu)